

Measurements of π^-p Elastic Scattering from 1.71 to 5.53 GeV/c*

M. FELLINGER, E. GUTMAN, R. C. LAMB, F. C. PETERSON, AND L. S. SCHROEDER

Institute for Atomic Research and Department of Physics, Iowa State University, Ames, Iowa 50010

AND

R. C. CHASE,† E. COLEMAN, AND T. G. RHOADES‡

School of Physics, University of Minnesota, Minneapolis, Minnesota 55455

(Received 1 June 1970)

The π^-p elastic scattering differential cross section has been obtained at 18 incident momenta from 1.71 to 5.53 GeV/c. The measurements were taken over a limited range of squared four-momentum transfer t near the forward direction. The statistical accuracy and resolution of these data are comparable to, or better than, existing data. The parameter b in the expression $d\sigma/dt = Ae^{bt}$ has been determined at each of our incident momenta, and a large ($\sim 25\%$) enhancement in b as a function of momentum is observed at a c.m. energy of ~ 2290 MeV. The relation of this bump in b with the well-established bump in the total π^-p cross section at ~ 2200 MeV is discussed.

I. INTRODUCTION

IN a recent experiment at the Argonne National Laboratory Zero-Gradient Synchrotron (ZGS), we measured the differential cross section for the elastic scattering of negative pions from deuterium at 2.01, 3.77, and 5.53 GeV/c.¹ To check the acceptance of our apparatus, we made measurements of the process $\pi^-p \rightarrow \pi^-p$ over a similar momentum range and compared them with existing π^-p elastic scattering measurements.²⁻⁴ In this paper we present the π^-p measurements. The measurements were made at 12 incident pion momenta in the range 1.71–2.76 GeV/c and also at 3.01, 3.52, 3.77, 4.02, 5.03, and 5.53 GeV/c. The closely spaced 1.71- to 2.76-GeV/c data were taken to help settle the question of what nucleon resonances are present in the mass region of the $N(2190)$.

Our data are in agreement with previous measurements,²⁻⁴ and in the 1.71- to 2.76-GeV/c region have somewhat superior statistical accuracy than previous results. These data coupled with polarization measurements of the same process⁴ have proven useful in providing additional evidence for a nucleon resonance in the H_{10} partial wave at a mass value of 2245 MeV.⁵ Our

data are confined to a limited angular region; in terms of t , the squared four-momentum transfer, the data cover a t interval of approximately -0.2 to -0.7 (GeV/c)².

Section II gives the details of our experimental method. Section III presents the differential cross sections in tabular form, as well as the momentum variation of the parameter b in the expression $d\sigma/dt = Ae^{bt}$. This exponential slope b shows about a 25% increase at c.m. energy of 2290 MeV, significantly higher in mass than the well-known bump in the π^-p total cross section near 2200 MeV.^{6,7}

II. EXPERIMENTAL METHOD

The experiment was performed in the 17° beam of the ZGS. The beam transport system determined the momentum of the pions to $\pm 1\%$ and brought the beam to a final focus on a 2.31-in.-long liquid-hydrogen target. The beam intensity varied in the range $1-7 \times 10^6$ pions/pulse, depending on the beam momentum, with a pulse repetition rate of 1000 pulses/h. The beam angular divergence was ± 5 mrad horizontally and ± 3 mrad vertically. The experimental apparatus used to detect the elastic events is shown in Fig. 1. The pion beam was detected by a series of scintillation counters labeled S_1, S_2, S_3 , and S_4 . Counters S_1 and S_2 are not shown in the figure and are located near the first focus of the 17° beam. The beam size was defined by S_4 , a $\frac{3}{4} \times \frac{3}{4}$ -in. counter.

Elastic events were detected in a double-arm spectrometer consisting of the two bending magnets $M1$ and $M2$ and scintillation counter arrays A, B , and P . Each of the A and B arrays consisted of 16 elements; the P array consisted of 30 elements. The dimensions for the A, B , and P elements are shown in Fig. 1. Negative particles traversed $M1$ and were detected by pairs of

* Work supported in part by the Ames Laboratory of the U. S. Atomic Energy Commission (Contribution No. 2762) and the National Aeronautics and Space Administration.

† Present address: American Science Engineering, Cambridge, Mass. 02142.

‡ Present address: Department of Physics, University of Birmingham, Edg Baston, Birmingham 15, England.

¹ M. Fellingner, E. Gutman, R. C. Lamb, F. C. Peterson, L. S. Schroeder, R. C. Chase, E. Coleman, and T. G. Rhoades, Phys. Rev. Letters **22**, 1265 (1969).

² C. T. Coffin, N. Dikmen, L. Ettliger, D. Meyer, A. Saulys, K. Terwilliger, and D. Williams, Phys. Rev. **159**, 1169 (1967).

³ W. Busza, B. G. Duff, D. A. Garbutt, F. F. Heymann, C. C. Nimmon, K. M. Potter, T. P. Swetman, E. H. Bellamy, T. F. Buckley, R. W. Dobinson, P. V. March, J. A. Strong, and R. N. F. Walker, Phys. Rev. **180**, 1339 (1969).

⁴ References to other π^-p elastic scattering data may be found in G. Giacomelli, P. Pini, and S. Stazni, CERN Report No. CERN/HERA 69-1 (unpublished), available in the U. S. A. from the Lawrence Radiation Laboratory, Berkeley, and in Europe from CERN, Geneva.

⁵ J. R. Hull and R. A. Leacock, following paper, Phys. Rev. D **1**, 1783 (1970).

⁶ A. N. Diddens, E. W. Jenkins, T. F. Kycia, and K. F. Riley, Phys. Rev. Letters **10**, 262 (1963).

⁷ A. A. Carter, K. F. Riley, R. J. Tapper, D. V. Bugg, R. S. Gilmore, K. M. Knight, D. C. Salter, G. H. Stafford, E. J. N. Wilson, J. D. Davies, J. D. Dowell, P. M. Hattersley, R. J. Homer, and A. W. O'Dell, Phys. Rev. **168**, 1457 (1968).

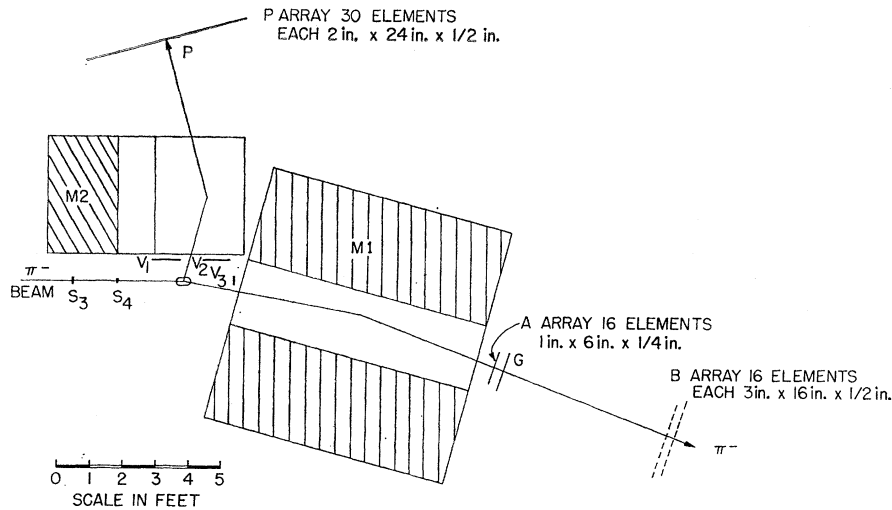


FIG. 1. Plan view of experimental apparatus. The pion beam is incident from the left on a hydrogen target. The scattered pions pass through magnet $M1$, and counter arrays A and B and are detected in coincidence with recoil protons in the side array P .

corresponding A and B elements. The width of an A array element determined the scattering-angle acceptance for each data point. The 16 pairs of corresponding A and B counters allowed 16 simultaneous

differential cross sections to be measured. A single scintillation counter G behind the A array determined the azimuthal angular acceptance. The recoil protons traversed $M2$ and were detected by the P array. The V_1 and V_2 counters were used to veto particles which did not satisfy the angular restrictions of πp elastic-scattering kinematics. The V_3 counter was used as an additional anticoincidence counter to veto beam pions that did not interact in the target. Events satisfying the following electronic coincidence requirements were selected and stored in a multichannel analyzer: (a) a count in beam counters ($S_1 S_2 S_3 S_4$), (b) no count in veto counters ($\bar{V}_1 \bar{V}_2 \bar{V}_3$), (c) a count in corresponding A and B counters in coincidence with a count in *any* of the P counters, and (d) a count in G . These events were sorted into 16 different groups corresponding to the 16 AB pairs. For each pair the distribution of events along the P array was obtained.

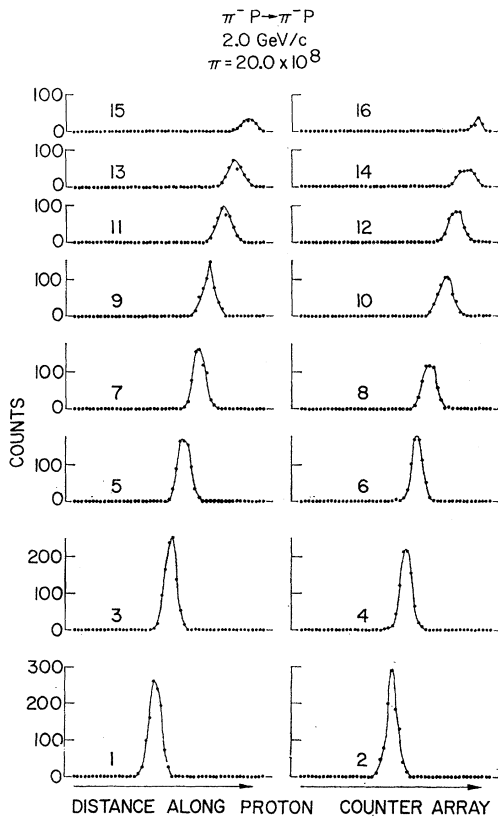


FIG. 2. Typical raw data run. The beam momentum is 2.01 GeV/c and the total number of incident pions is 20×10^8 . There are 16 event distributions shown in the figure; increasing number means increasing pion scattering angle. The elastic events form a well-defined peak with a background of less than 1%.

TABLE I. Summary of experiment.

Incident momentum (GeV/c)	$ t $ range covered (GeV/c) ²	Statistical accuracy of data (%)
1.71	0.17-0.37	5.0- 6.0
1.81	0.19-0.41	3.0- 5.5
1.91	0.24-0.45	3.5- 7.0
2.01	0.24-0.49	3.5- 8.0
2.09	0.26-0.53	3.5- 8.5
2.16	0.27-0.56	2.0- 7.0
2.23	0.29-0.60	3.5-15.0
2.31	0.31-0.64	3.5-11.5
2.41	0.34-0.69	3.5-12.5
2.51	0.36-0.74	4.0-13.0
2.62	0.39-0.80	3.0-10.0
2.76	0.43-0.88	5.0-14.0
3.01	0.51-0.88	6.0-10.0
3.52	0.29-0.57	4.5-12.0
3.77	0.24-0.56	4.0-13.0
4.02	0.27-0.55	4.0- 9.5
5.03	0.27-0.63	3.5-10.0
5.53	0.28-0.62	3.5- 9.5

TABLE II. π^-p elastic scattering.

$-t$ (GeV/c) ²	$d\sigma/dt$ (mb/(GeV/c) ²)	Statistical error (mb/(GeV/c) ²)	$-t$ (GeV/c) ²	$d\sigma/dt$ (mb/(GeV/c) ²)	Statistical error (mb/(GeV/c) ²)	$-t$ (GeV/c) ²	$d\sigma/dt$ (mb/(GeV/c) ²)	Statistical error (mb/(GeV/c) ²)
1.71 GeV/c			2.09 GeV/c			2.41 GeV/c		
0.177	17.87	0.99	0.292	6.52	0.23	0.340	4.42	0.16
0.188	16.10	0.91	0.309	5.63	0.21	0.361	3.53	0.14
0.199	14.61	0.85	0.326	4.86	0.19	0.382	2.74	0.12
0.211	14.15	0.82	0.343	4.32	0.18	0.403	2.54	0.12
0.235	11.88	0.73	0.360	3.38	0.16	0.425	2.00	0.10
0.259	9.36	0.34	0.378	2.98	0.14	0.448	1.56	0.09
0.285	7.29	0.29	0.396	2.52	0.13	0.470	1.17	0.07
0.299	6.63	0.28	0.415	2.06	0.12	0.493	0.914	0.065
0.312	5.95	0.26	0.434	1.81	0.11	0.516	0.801	0.060
0.325	5.64	0.26	0.453	1.35	0.09	0.540	0.637	0.053
0.339	4.98	0.24	0.472	1.54	0.10	0.563	0.533	0.047
0.367	4.16	0.23	0.491	1.19	0.09	0.587	0.349	0.039
			0.511	0.958	0.080	0.611	0.376	0.040
			0.530	0.967	0.081	0.637	0.352	0.039
						0.661	0.272	0.035
						0.685	0.287	0.036
1.81 GeV/c			2.16 GeV/c			2.51 GeV/c		
0.197	13.61	0.42	0.277	7.28	0.16			
0.210	12.78	0.40	0.293	6.29	0.15	0.367	3.66	0.14
0.222	12.47	0.39	0.311	5.06	0.13	0.390	3.03	0.13
0.235	11.03	0.36	0.329	4.61	0.12	0.413	2.44	0.11
0.248	9.52	0.33	0.346	3.63	0.11	0.435	2.02	0.10
0.262	8.35	0.30	0.364	3.26	0.10	0.459	1.60	0.09
0.275	7.52	0.28	0.383	2.62	0.09	0.482	1.28	0.08
0.289	7.62	0.28	0.402	2.32	0.08	0.506	1.10	0.07
0.303	6.26	0.25	0.421	1.81	0.07	0.531	0.839	0.060
0.317	6.05	0.24	0.441	1.58	0.06	0.556	0.600	0.049
0.332	5.06	0.22	0.462	1.30	0.06	0.581	0.554	0.047
0.346	4.78	0.21	0.481	1.10	0.05	0.607	0.518	0.045
0.361	4.14	0.20	0.501	0.948	0.050	0.632	0.389	0.039
0.376	3.73	0.19	0.522	0.805	0.046	0.659	0.347	0.037
0.392	3.54	0.18	0.542	0.658	0.042	0.685	0.268	0.033
0.407	3.09	0.17	0.563	0.606	0.041	0.711	0.235	0.031
						0.738	0.249	0.032
1.91 GeV/c			2.23 GeV/c			2.62 GeV/c		
0.247	10.12	0.35	0.293	6.11	0.25	0.396	3.11	0.10
0.260	9.00	0.32	0.312	5.23	0.22	0.420	2.46	0.09
0.275	7.60	0.29	0.330	4.41	0.20	0.444	2.12	0.08
0.290	7.01	0.28	0.348	3.67	0.18	0.468	1.64	0.07
0.304	6.18	0.25	0.368	3.07	0.16	0.494	1.26	0.06
0.320	5.51	0.24	0.387	2.75	0.15	0.520	1.02	0.05
0.335	4.68	0.21	0.406	1.99	0.12	0.546	0.784	0.047
0.351	4.36	0.20	0.427	1.80	0.12	0.572	0.680	0.043
0.367	4.00	0.19	0.468	1.27	0.10	0.598	0.548	0.038
0.383	3.49	0.18	0.489	1.00	0.08	0.626	0.435	0.033
0.400	3.16	0.17	0.510	0.845	0.077	0.653	0.407	0.032
0.416	2.75	0.16	0.531	0.637	0.068	0.681	0.297	0.027
0.433	2.17	0.15	0.553	0.574	0.065	0.708	0.262	0.026
0.450	1.99	0.14	0.574	0.495	0.061	0.736	0.287	0.027
			0.596	0.346	0.051	0.764	0.276	0.027
						0.792	0.285	0.028
2.01 GeV/c			2.31 GeV/c			2.76 GeV/c		
0.241	9.19	0.31	0.314	5.29	0.18	0.439	1.98	0.10
0.256	8.49	0.29	0.333	4.14	0.16	0.466	1.71	0.09
0.271	7.97	0.27	0.352	3.53	0.14	0.493	1.35	0.08
0.287	6.33	0.24	0.373	2.99	0.13	0.520	0.965	0.063
0.303	5.99	0.23	0.393	2.33	0.11	0.547	0.863	0.059
0.318	5.18	0.21	0.413	2.01	0.10	0.576	0.758	0.054
0.335	4.25	0.18	0.434	1.64	0.09	0.605	0.582	0.047
0.352	3.79	0.17	0.456	1.41	0.08	0.633	0.467	0.041
0.369	2.99	0.15	0.477	1.20	0.08	0.663	0.394	0.037
0.386	3.03	0.15	0.499	0.939	0.066	0.692	0.339	0.034
0.404	2.56	0.13	0.522	0.723	0.057	0.723	0.339	0.034
0.421	2.01	0.12	0.544	0.632	0.054	0.753	0.291	0.032
0.439	1.94	0.12	0.566	0.542	0.050	0.783	0.340	0.034
0.457	1.87	0.12	0.589	0.456	0.046	0.813	0.241	0.029
0.475	1.60	0.11	0.612	0.339	0.040	0.844	0.219	0.028
0.494	1.23	0.10	0.636	0.369	0.042	0.875	0.196	0.027
2.09 GeV/c								
0.260	8.36	0.28						
0.276	6.99	0.25						

TABLE II. (continued)

$-t$ (GeV/c) ²	$d\sigma/dt$ (mb/(GeV/c) ²)	Statistical error (mb/(GeV/c) ²)	$-t$ (GeV/c) ²	$d\sigma/dt$ (mb/(GeV/c) ²)	Statistical error (mb/(GeV/c) ²)	$-t$ (GeV/c) ²	$d\sigma/dt$ (mb/(GeV/c) ²)	Statistical error (mb/(GeV/c) ²)
3.01 GeV/c			3.52 GeV/c			4.02 GeV/c		
0.515	1.20	0.07	0.527	0.734	0.078	0.457	1.82	0.12
0.545	1.00	0.06	0.563	0.675	0.076	0.499	1.02	0.09
0.577	0.755	0.052				0.541	0.736	0.074
0.608	0.611	0.046	3.77 GeV/c			5.03 GeV/c		
0.639	0.496	0.041	0.240	7.60	0.30	0.274	5.73	0.18
0.672	0.435	0.038	0.270	6.45	0.27	0.316	4.67	0.15
0.706	0.364	0.034	0.302	5.52	0.24	0.363	3.03	0.12
0.739	0.334	0.032	0.335	4.13	0.20	0.410	2.04	0.09
0.773	0.283	0.029	0.369	3.26	0.17	0.461	1.38	0.08
0.808	0.266	0.028	0.404	2.47	0.15	0.514	0.804	0.055
0.842	0.259	0.027	0.441	2.01	0.13	0.570	0.635	0.048
0.876	0.275	0.028	0.479	1.17	0.10	0.627	0.354	0.035
			0.517	0.757	0.077	5.53 GeV/c		
			0.557	0.536	0.065	0.281	5.28	0.16
3.52 GeV/c			4.02 GeV/c			0.328	4.11	0.14
0.294	5.92	0.26	0.273	6.54	0.26	0.379	2.62	0.11
0.324	4.66	0.22	0.306	4.88	0.22	0.434	1.94	0.09
0.355	3.20	0.18	0.342	4.20	0.19	0.492	1.16	0.07
0.388	2.60	0.16	0.379	2.89	0.16	0.553	0.692	0.049
0.421	2.00	0.14	0.417	2.25	0.13	0.614	0.385	0.036
0.456	1.38	0.11						
0.491	1.02	0.10						

Figure 2 shows some typical data accumulated for a beam momentum of 2.01 GeV/c. There are 16 separate distributions labelled 1-16, corresponding to increasing pion scattering angle. In each of the distributions the elastic-scattering events appear as a peak with a background of less than 1%. Since the acceptance of our apparatus varies slowly with angle, one can roughly see in Fig. 2 the variation in the differential cross section as a function of pion scattering angle. Also one can see the variation in the recoil proton direction. The data were displayed in this manner simultaneously with the running of the experiment so that any trouble that developed would have been readily detected. It took 6 h

to accumulate the data shown in Fig. 2. These particular data are all of the data at 2.01 GeV/c. The positions of the elastic peaks agree with predictions of a Monte Carlo simulation of the experiment.

III. RESULTS

The differential cross section for a particular scattering angle interval associated with an element of the A array is given by the formula

$$d\sigma/dt = E/N_\pi N_p \Delta t,$$

where E is the number of events, N_π is the number of incident pions, N_p is the number/cm² of target protons, and Δt is the interval of the squared momentum transfer associated with the instrumental solid angle. The number of events was determined from the counts in the elastic peak with a typical 1% subtraction of background determined from target empty running. The number of beam pions was determined from the number of beam counts, $S_1 S_2 S_3 S_4$. The number of protons/cm² was determined from a knowledge of the length of the target and the known density of liquid hydrogen at an operating pressure of 1 atm. Δt is given by the formula

$$\Delta t = (q^2/\pi) \Delta\Omega_{c.m.},$$

where q is the c.m. momentum and $\Delta\Omega_{c.m.}$ is the c.m. solid angle associated with the particular element of the A array struck. The instrumental solid angle was calculated by hand and by a Monte Carlo computer program, in which the effects of finite beam divergence, beam size, and multiple scattering were taken into account. These effects were ignored in our hand calculation of $\Delta\Omega$. The difference between the hand calculation

TABLE III. Parameter b in $d\sigma/dt = A e^{bt}$, from a fit to the present data for t values $|t| \leq 0.63$ (GeV/c)².

Beam momentum (GeV/c)	Number of data points	χ^2	b (GeV/c) ⁻²
1.71	12	6.2	7.91±0.25
1.81	16	16.5	7.30±0.16
1.91	14	7.0	7.76±0.21
2.01	16	23.2	8.02±0.16
2.09	16	21.6	8.55±0.16
2.16	16	17.2	9.08±0.11
2.23	15	4.9	9.24±0.21
2.31	15	6.7	9.06±0.18
2.41	13	11.6	9.63±0.21
2.51	11	7.2	8.81±0.24
2.62	10	4.4	8.73±0.22
2.76	7	5.1	7.53±0.44
3.01	4	0.3	7.40±0.96
3.52	9	5.4	8.64±0.28
3.77	10	28.6	7.77±0.21
4.02	8	12.0	7.70±0.25
5.03	8	12.9	7.93±0.17
5.53	7	13.2	7.50±0.18

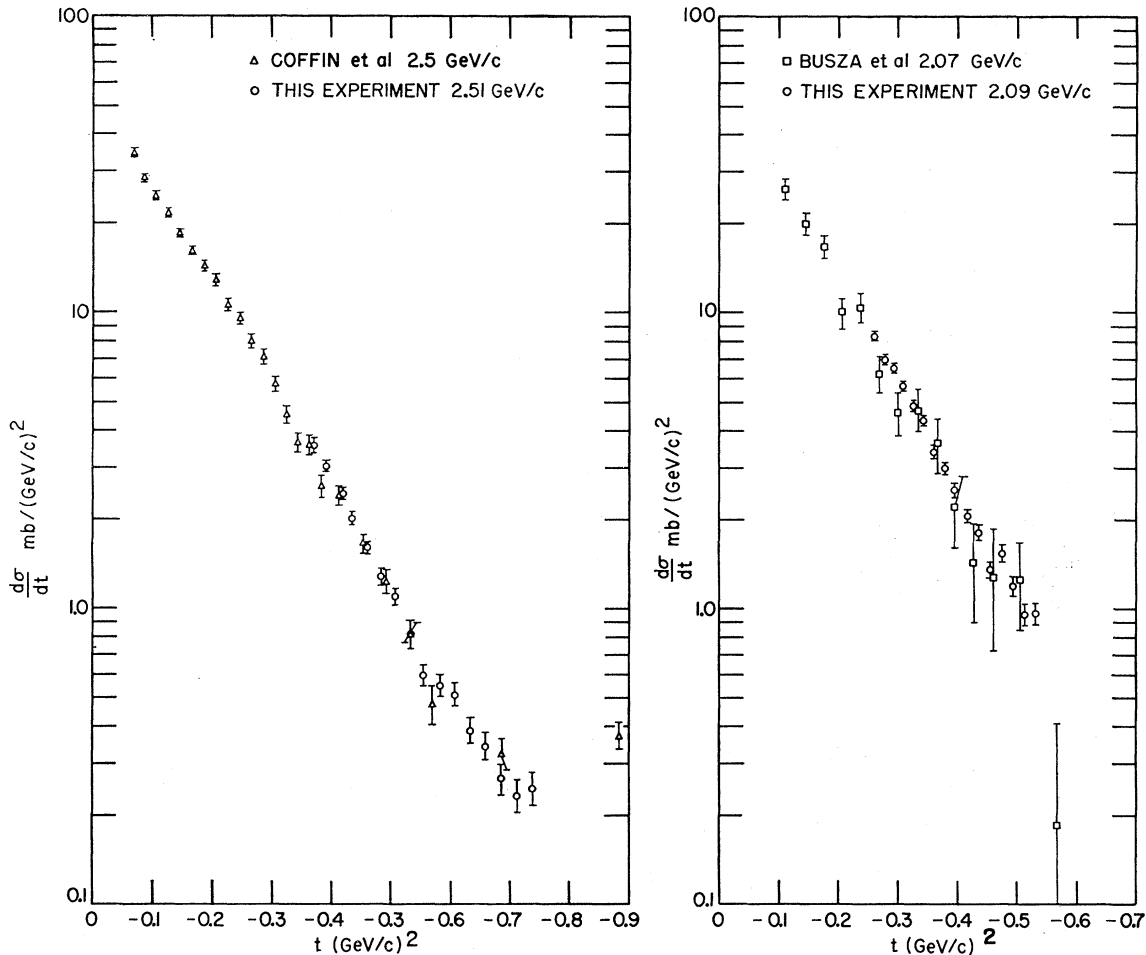


FIG. 3. Comparison of our data from other experiments near 2.5 and 2.1 GeV/c.

and the Monte Carlo calculation was about one part in a few hundred and the Monte Carlo results were used. The t value associated with a particular A array element was also calculated by hand and by the Monte Carlo program. Again differences were slight, and the Monte Carlo program values were used.

Corrections were applied to the data for muon and electron contamination of the pion beam, for decay of the scattered pion, for electronic deadtime effects due to V_1 , V_2 , and V_3 , and for absorption of particles in scintillators, liquid hydrogen, and other material. The combined correction due to these effects was typically 20%.

Table I lists the 18 momenta at which the experiment was performed, the t range covered⁸ at each

⁸ The measurements from 1.71 to 2.76 GeV/c were made with the bending magnet $M1$ at a fixed angle of 25° with respect to the incident beam line. The magnet current was set to bend a particle with the beam momentum through 10° at each momentum. Consequently, with the fixed bend angle and approximately fixed counter positions at each run, the t range covered at each momentum moved to larger values of t as the beam momentum increased, as indicated in Table 1

momentum, and the statistical accuracy of the differential cross sections. The elastic differential cross sections for the 18 momenta are tabulated in Table II along with their associated errors. The quoted errors are statistical errors associated with event counts only. The relative normalization error between any two of our data sets at different momenta is less than 2%. In addition there is an over-all absolute uncertainty of $\pm 5\%$ to be uniformly associated with all data points.

The present data have been compared with other measurements²⁻⁴ at the same or nearby momenta and are in good agreement. The extent of this agreement as well as the quality of our data is illustrated in Fig. 3, where we have plotted our data at two momenta and data from other experiments at similar momenta.

In an effort to arrive at a simplified understanding of these cross-section measurements we have fitted the differential cross sections at each momentum to an expression of the form

$$d\sigma/dt = Ae^{bt},$$

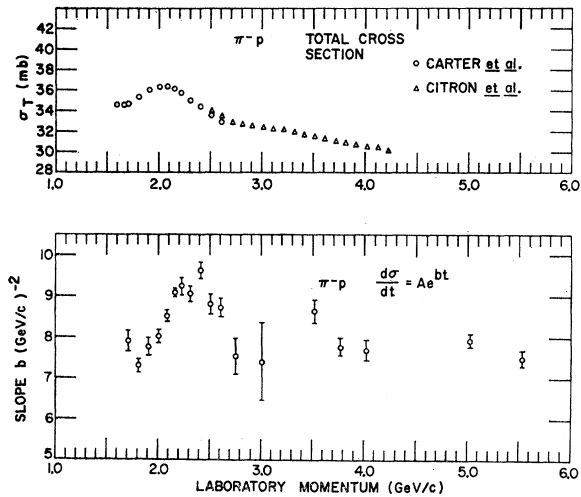


FIG. 4. In the lower portion: slope parameter b versus laboratory beam momentum; in the upper portion: total π^-p cross section versus laboratory beam momentum. The values of b plotted are taken exclusively from this experiment. The values of σ_T plotted are taken from Carter *et al.* (Ref. 7) and Citron *et al.* (Ref. 10).

a form suggested by a small-angle approximation to an optical model of high-energy scattering⁹ and employed extensively to parametrize small-angle scattering data. A least-squares fitting procedure determined the coefficients A and b at each of the 18 momenta. In order to arrive at reasonable χ^2 's, it was necessary to restrict the fit to data points for which $|t| \leq 0.63$ (GeV/c)². Beyond this value of t the differential cross section has a secondary peak or "shoulder" and deviates drastically from a simple exponential dependence on t . All of our data points for which $|t| \leq 0.63$ (GeV/c)² were used; therefore, the t range of the fits is somewhat momentum dependent. The values of b obtained from this procedure are listed in Table III and plotted in the lower half of Fig. 4. In the upper half of Fig. 4, we have plotted the π^-p total cross section taken from Carter *et al.*⁷ and from Citron *et al.*¹⁰ Note the large bump in b (approximately 25%) in the vicinity of the $\sim 8\%$ bump in the total cross section, usually attributed to the $N(2190)$ $J^P = \frac{7}{2}^-$. The central position of the bump in b is at a value of $p_{\text{lab}} \approx 2.3$ GeV/c while the position of the bump in σ_T is at a value of $p_{\text{lab}} \approx 2.1$ GeV/c. The

⁹ See, e.g., lectures by A. M. Wetherell on high-energy scattering, CERN Report No. CERN 65-24 (unpublished); and M. L. Perl, L. W. Jones, and C. C. Ting, Phys. Rev. **132**, 1252 (1963).

¹⁰ A. Citron, W. Galbraith, T. F. Kycia, B. A. Leontic, R. H. Phillips, A. Rousset, and P. H. Sharp, Phys. Rev. **144**, 1101 (1966).

corresponding c.m. energies at these momenta are ≈ 2290 and ≈ 2200 MeV, respectively. We would like to make the following two points: First, the bump in b is due to the presence of direct-channel resonances. The evidence for the correlation of variations in b with direct-channel resonances has been extensively presented by Lasinski, Levi Setti, and Predazzi.¹¹ Second, the shift in the position of the bump from ~ 2200 MeV in σ_T to ~ 2290 MeV in b can be understood in terms of the simple phenomenological model used in Ref. 11. In this model the scattering amplitude at small angles has two contributions, one due to diffraction scattering and the second due to direct-channel resonance formation. As a consequence of this model, Lasinski *et al.* demonstrate that resonances of different spin contribute to structure in b with a relative weight which is different than the relative weight with which they contribute to structure in σ_T . For a given resonance elasticity the weighting factor increases with increasing spin more rapidly for b than for σ_T . Therefore, one qualitative explanation for the mass difference in the positions of the bumps is that there are several resonances of different spin in this mass region, and the higher-spin resonances have greater mass. A similar, but more precise, conclusion is reached by the authors of Ref. 5. Their detailed examination of our data and polarization data⁴ provides evidence for two nucleon resonances in this energy region: one at 2245 MeV in the H_{19} partial wave, and one at 2260 MeV in the G_{17} partial wave. This latter resonance is the familiar $N(2190)$. As the authors of Ref. 5 demonstrate, the bump in the total cross section at a mass value of 2200 MeV is due to these two high-spin resonances plus the $D_{13}(2040)$ resonance.

ACKNOWLEDGMENTS

We appreciate the fine technical support offered by the Zero-Gradient Synchrotron personnel, in particular Tony Passi. We thank Dr. R. A. Lundy for a very helpful experimental suggestion, Professor A. D. Krisch for suggesting the measurements in the region of the $N(2190)$, and Professor R. A. Leacock for useful discussions. We appreciate the assistance of P. N. Scharbach, G. Mrozek, and T. Curtright during part of the experiment. We also appreciate the capable technical help of Stephen Mosher and William Glass of Ames Laboratory.

¹¹ T. Lasinski, R. Levi Setti, and E. Predazzi, Phys. Rev. **179**, 1426 (1969).